

Sewage, Salt, Silica, and SARS-CoV-2 (4S): An Economical Kit-Free Method for Direct Capture of SARS-CoV-2 RNA from Wastewater

Oscar N. Whitney, Lauren C. Kennedy, Vinson B. Fan, Adrian Hinkle, Rose Kantor, Hannah Greenwald, Alexander Crits-Christoph, Basem Al-Shayeb, Mira Chaplin, Anna C. Maurer, Robert Tjian, and Kara L. Nelson*



Cite This: *Environ. Sci. Technol.* 2021, 55, 4880–4888



Read Online

ACCESS |



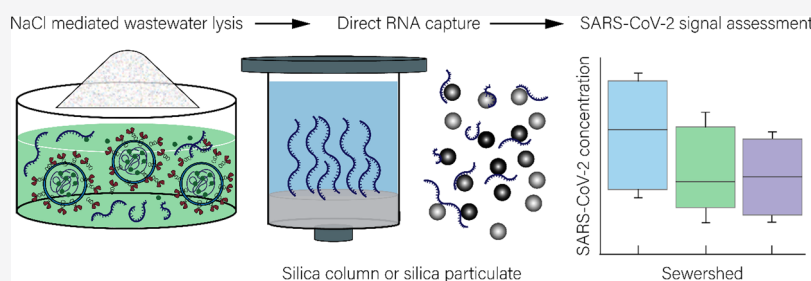
Metrics & More



Article Recommendations



Supporting Information



ABSTRACT: Wastewater-based epidemiology is an emerging tool to monitor COVID-19 infection levels by measuring the concentration of severe acute respiratory syndrome coronavirus 2 (SARS-CoV-2) RNA in wastewater. There remains a need to improve wastewater RNA extraction methods' sensitivity, speed, and reduce reliance on often expensive commercial reagents to make wastewater-based epidemiology more accessible. We present a kit-free wastewater RNA extraction method, titled "Sewage, Salt, Silica and SARS-CoV-2" (4S), that employs the abundant and affordable reagents sodium chloride (NaCl), ethanol, and silica RNA capture matrices to recover sixfold more SARS-CoV-2 RNA from wastewater than an existing ultrafiltration-based method. The 4S method concurrently recovered pepper mild mottle virus (PMMoV) and human 18S ribosomal subunit rRNA, which have been proposed as fecal concentration controls. The SARS-CoV-2 RNA concentrations measured in three sewersheds corresponded to the relative prevalence of COVID-19 infection determined via clinical testing. Lastly, controlled experiments indicate that the 4S method prevented RNA degradation during storage of wastewater samples, was compatible with heat pasteurization, and in our experience, 20 samples can be processed by one lab technician in approximately 2 h. Overall, the 4S method is promising for effective, economical, and accessible wastewater-based epidemiology for SARS-CoV-2, providing another tool to fight the global pandemic.

INTRODUCTION

Wastewater-based epidemiology (WBE) enables the indirect assessment of viral infection prevalence in populations.^{1–3} The quantity of viral nucleic acids shed into wastewater by infected individuals, whether symptomatic or not, serves as a proxy for the relative prevalence of infection.¹ WBE can provide population-level infection information for up to many thousands of individuals in a community to complement individual-level testing and aid public health decision making.⁴

WBE is now being applied to monitor and even predict population-level coronavirus disease 2019 (COVID-19) outbreaks.^{1,5} Local COVID-19 prevalence is difficult to assess due to insufficient individual testing capacity, rendering effective response more challenging.⁶ Wastewater can provide insights into COVID-19 prevalence, as COVID-19 patients shed SARS-CoV-2 RNA in their stool and thus into wastewater.^{7,8} Emerging studies report wastewater SARS-CoV-2 concentrations that correspond to reported clinical prevalence of COVID-19, with potential for early detection of COVID-19

outbreaks and identification of newly emerging SARS-CoV-2 variants.^{9–12} To extract and quantify the concentration of SARS-CoV-2 RNA shed into wastewater, researchers are using size- and charge-based concentration methods that concentrate intact SARS-CoV-2 virus prior to RNA extraction.^{13–15} These methods employ a primary concentration step via sieving by particle size, enmeshment of viral particles in precipitates that can be separated by mass, or adsorption via electrostatic interactions, prior to RNA extraction.¹⁵ These methods can be relatively time-consuming and become inaccessible if they are dependent on reliable supply of commercial reagents, a paucity of which has already hampered clinical SARS-CoV-2 testing

Received: December 1, 2020

Revised: March 1, 2021

Accepted: March 11, 2021

Published: March 24, 2021



efforts.^{13–17} Furthermore, the use of primary concentration assumes the recovery of intact virus and is therefore not geared toward cocapturing RNA from SARS-CoV-2 viruses that have already lysed or capture of nonviral RNAs suitable as fecal concentration controls. Lastly, current CDC safety guidelines recommend a biosafety level 2 facility with unidirectional airflow and BSL-3 precautions when employing environmental sampling procedures that concentrate viruses presumed to be intact.¹⁸ To mitigate concerns of concentrating potentially infectious virus, heat-based wastewater sample pasteurization and subsequent extraction could allow for easier and safer wastewater processing after collection.

We aimed to develop an economical, kit-free method for the direct capture (extraction) of SARS-CoV-2 RNA from wastewater. The resulting method, described herein, employs lysis of biological particles via sodium chloride (NaCl), heat-based pasteurization, coarse filtration, ethanol precipitation, and RNA capture via silica-based columns (4S-column) or silicon dioxide slurry (4S-Milk-of-Silica). This approach was developed with the aim to provide recovery of wastewater RNA without mass, size, or charge bias, the ability to cocapture RNA from intact and lysed SARS-CoV-2 virus, as well as RNA from other biological particles in wastewater that are suitable as fecal concentration controls, such as pepper mild mottle virus (present in dietary peppers and shed in feces) and human 18S ribosomal RNA.¹⁹ As compared to other wastewater RNA extraction procedures, the 4S method is to our knowledge the only procedure to simultaneously concentrate and extract RNA from a large volume (40–400 mL) of wastewater, enabling the processing of 20 wastewater samples by one lab technician within approximately 2 h.

The 4S method was evaluated in terms of its sensitivity to detect wastewater SARS-CoV-2 and ability to remove RT-qPCR inhibitors. Furthermore, we assessed whether the lysis salts added to wastewater during the 4S method could also protect wastewater RNA from degradation. We found that 4S method's omission of a primary concentration step and extraction from a relatively large wastewater volume (40 mL) allowed for highly sensitive, same-day measurement of wastewater SARS-CoV-2 abundance and removal of RT-qPCR inhibitors. Furthermore, the sodium chloride and ethylenediaminetetraacetic acid (EDTA) lysis additives served to protect wastewater RNA from degradation. Lastly, we found that the 4S method was compatible with heat pasteurization, which makes wastewater samples safer to process.

MATERIALS AND METHODS

Sample Collection. For this study, we obtained composite 24 h wastewater influent samples from East Bay Municipal Utility District's wastewater treatment plant. These samples represent three discrete sampling areas: North and West Berkeley, El Cerrito, Kensington, and Albany (subsewershed "N"), Oakland/Piedmont (subsewershed "S"), and Berkeley/Oakland Hills (subsewershed "A") (interceptor coverage detailed in Figure S2A). Samples processed via the 4S-column method and ultrafiltration were kept at 4 °C on ice during transport and processed within 24 h. Samples processed via the "Milk-of-Silica" procedure were kept at –80 °C and processed within two weeks. Biological replicates were defined as aliquots of the same wastewater sample, processed independently through the entire method. For example, three aliquots from the same wastewater were processed via the 4S-column method.

Wastewater RNA Extraction. Wastewater RNA extraction via the 4S-column and 4S-Milk-of-Silica methods is detailed in depth at <https://www.protocols.io/view/v-4-direct-wastewater-rna-capture-and-purification-bpdfmi3n> and [dx.doi.org/10.17504/protocols.io.biwfkfbn](https://doi.org/10.17504/protocols.io.biwfkfbn).^{20,21} For 4S RNA extraction using a silica column (4S-column), samples were lysed via the addition of sodium chloride (NaCl) to a final concentration of 4 M and EDTA to a final concentration of 1 mM and buffered via the addition of tris(hydroxymethyl)-aminomethane pH 7.2 to a final concentration of 10 mM. Bovine coronavirus vaccine stock (Bovilis Coronavirus Calf Vaccine, Merck Animal) was resuspended in 2 mL of PBS, diluted in PBS at a 1:10 ratio, and 50 μ L of diluted BCoV vaccine was added to each sample as a process control. Samples were heat-inactivated in a water bath (unless indicated otherwise) at 70 °C for 45 min and filtered using a 5 μ M DuraPore PVDF filter membrane (Millipore Sigma) and syringe filter. Ethanol was added to the sample filtrate to a final concentration of 35%. Samples were passed through Zymo-IIIP silica columns (Zymo Research) using a vacuum manifold. For all experiments other than the wash buffer tests (Figure 4, Supporting Information Figure S4), samples were washed with 25 mL of high NaCl (1.5 M) and ethanol (20%) containing wash buffer #1 (4S-WB1) and 50 mL of low NaCl (100 mM) and ethanol (80%) containing wash buffer #2 (4S-WB2). Columns were detached from the vacuum manifold and centrifuged at 10,000 g for 2 min to remove any residual 4S-WB2 present in the column. Washed RNA was eluted from silica columns using 200 μ L of ZymoPURE elution buffer (Zymo Research) preheated to 50 °C and eluted from the final step of the "Milk-of-Silica" procedure using pH 8 Tris-EDTA buffer preheated to 50 °C. Eluted RNA was stored at 4 °C for same-day use or frozen at –80 °C for later use and storage.

For 4S-Milk-of-Silica extraction, samples were lysed, heat inactivated, and filtered as in the 4S-column extraction. Next, a 1 g/mL silicon dioxide slurry in water was added to the filtered lysate and incubated at room temperature for 10 min. The lysate and silica slurry were centrifuged at 4000 \times g for 5 min, pelleting wastewater RNA bound to silica particulates. The lysate supernatant was decanted, and the silica pellet was washed with 40 mL 4S-WB1 and 40 mL of 4S-WB2 via centrifugation and wash buffer decanting. The washed silica pellet was resuspended in 20 mL of pure water preheated to 37 °C to elute bound RNA. Next, the silicon dioxide particulate was pelleted via centrifugation and the eluted RNA was separated and concentrated via isopropanol precipitation, as previously described.^{21,22} Here, 20 mL of 100% volume isopropanol and 4 mL of 3 M pH 5.2 sodium acetate were added to the eluted RNA. The mixture was centrifuged for 4000 \times g in a swinging bucket rotor for 1 h, forming a semitranslucent RNA pellet. The excess supernatant was decanted from the RNA pellet, and the pellet was washed with 40 mL of 75% volume ethanol by vortexing the pellet until fully suspended. The pellet was reprecipitated via centrifugation at 4000 \times g for 30 min and excess ethanol was decanted from the RNA pellet. The washed pellet was resuspended in 1 mL 75% ethanol, transferred to a 1.5 mL tube, and precipitated via centrifugation at 5000 \times g for 5 min. Excess ethanol was carefully aspirated from the pellet and the pellet was dried via incubation at 37 °C for 10 min. The dried pellet was resuspended in 200 μ L of pH 8 TE buffer and stored at 4 °C for same-day use or frozen at –80 °C for later use and

storage. The 4S-column and 4S-Milk-of-Silica reagent costs are listed in Supporting Information Table S6.

For sample RNA concentration via ultrafiltration, Amicon 100-kDa ultrafilters (Millipore Sigma) were pretreated to block virus adsorption using 2 mL bovine serum albumin 1% (w/v) in 1 × PBS and then washed with PBS. Wastewater samples were divided into 40 mL aliquots and solids were removed via slow centrifugation with a swinging bucket rotor at 4700 × g for 30 min. The supernatant was decanted and passed through a 0.2 μm flat membrane filter (Steriflip, EMD Millipore). The filtrate was loaded onto the ultrafilter in increments of up to 15 mL and ultrafilters were spun for 10 min at 4700 × g for each increment. Flow-through was discarded and samples were concentrated until they were reduced to a final volume of ~250 μL. RNA was extracted from the ultrafiltration concentrate using an AllPrep DNA/RNA Mini kit (QIAGEN) following manufacturer instructions.

RNA Detection and Quantification Via RT-qPCR. This study employed four primer/probe sets: the SARS-CoV-2 N1 assay, pepper mild mottle virus (PMMoV) coat protein gene assay, bovine coronavirus transmembrane protein gene assay, and a newly developed human 18S ribosomal rRNA assay. (Supporting Information, Table S3) RT-qPCR reaction conditions are detailed in Table S1, assay thermocycling conditions are detailed in Table S2, and primer sequence information is in Table S3. RT-qPCR assay performance is detailed in Table S4 (validation) and Table S5 (limit of detection). Three technical replicate RT-qPCR wells were analyzed for each sample and standard. After outlier detection and removal, the arithmetic mean of C_q values for the technical replicates was determined; this value was used to determine the concentration for each biological replicate. RT-qPCR minimum information for publication of quantitative real-time PCR experiment (MIQE) documentation is detailed in Table S7. RT-qPCR analysis is detailed in the Supporting Information. Full data set and associated code are available in the Supporting Information as well as through Zenodo at DOI 10.5281/zenodo.4570691.

RESULTS AND DISCUSSION

Many current methods of wastewater viral RNA extraction assume that most viral particles within wastewater are intact and that the concentration of these intact viruses prior to extraction is necessary to achieve sensitive detection of SARS-CoV-2 in wastewater. Given this assumption, these methods typically employ precipitation-, charge-, or size-based viral concentration and subsequent RNA extraction of unpasteurized wastewater to preserve viruses in an intact state.^{14,15} Despite concentration, some methods were shown to recover as little as 0–1% of SARS-CoV-1 from wastewater during the SARS-CoV-1 epidemic.²³ We hypothesized that direct extraction could avoid loss of virus during the primary concentration step, and we therefore designed the 4S (sewage, salt, silica, and SARS-CoV-2) method to lyse viruses and microorganisms present in wastewater using sodium chloride and subsequently capture the free RNA using a silica RNA-binding matrix.

Direct Wastewater RNA Extraction Via the 4S Method. To benchmark the performance of the 4S method, we analyzed a 24 h composite wastewater sample treated with and without heat pasteurization and compared the recovery of endogenous SARS-CoV-2 to that of an ultrafiltration-based method. In addition, we compared the recovery of endogenous

PMMoV RNA, which may be useful to control for variable fecal concentrations in wastewater, and a spiked-in bovine coronavirus vaccine (BCoV), used as an RNA extraction process control (Figure 1). We observed that the 4S-column method recovered sixfold more SARS-CoV-2 RNA than ultrafiltration (Figure 1).

Surprisingly, SARS-CoV-2 recovery by the 4S method was not impacted by heat pasteurization, suggesting that further SARS-CoV-2 virus lysis did not occur. This result may imply that a large fraction of SARS-CoV-2 RNA was not bound to

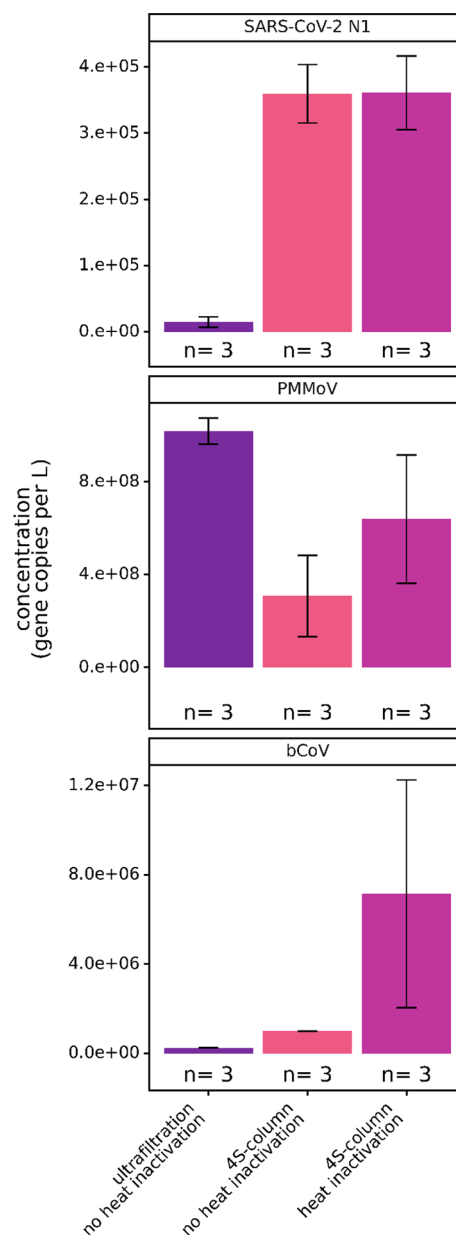


Figure 1. Comparison of SARS-CoV-2, PMMoV, and BCoV spike-in assay signals in gene copies per liter between the 4S-column method with and without heat inactivation and ultrafiltration. “n” represents the number of wastewater biological replicates per condition. Bars are plotted at the arithmetic mean of biological replicates and error bars represent the variation associated with biological triplicates as quantified by the arithmetic standard deviation of the biological triplicates.

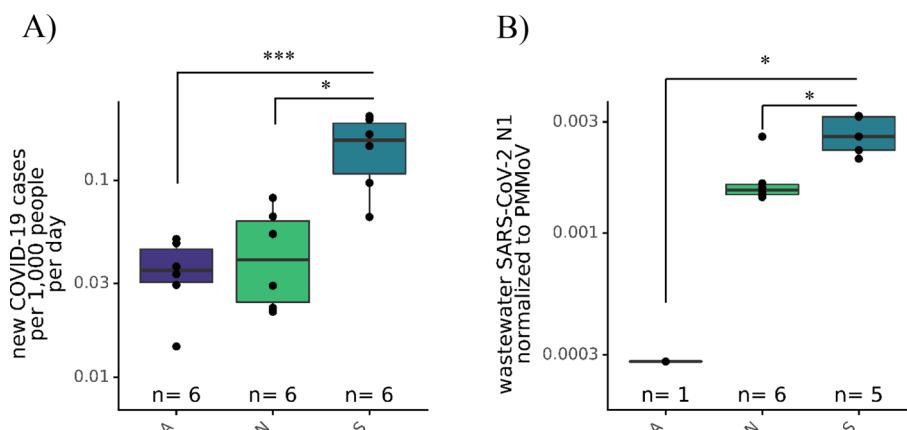


Figure 2. (A) New COVID-19 clinical cases per day per 100,000 population in three areas served by the distinct A, N, and S wastewater interceptors over 6 days from 7/15 to 7/21. “n” represents the number of days during which clinical case data were collected. (B) Comparison of SARS-CoV-2 N1 assay represented as SARS-CoV-2 gene copies per liter normalized to PMMoV gene copies per liter between interceptors serving the A, N, and S East Bay areas. “n” represents the number of biological replicates (the wastewater was collected on a single day in the 6-day window). The Kruskal-Wallis test followed by Dunn’s test was performed to determine significance, where * = $p < 0.05$ and *** = $p < 0.001$.

virus particles; this unbound RNA was captured by the 4S method but was not efficiently concentrated by ultrafiltration.

The 4S-column method without heat pasteurization also recovered sixfold more BCoV than ultrafiltration and 28-fold more BCoV with heat pasteurization. In this case, heat pasteurization may promote additional lysis of encapsidated BCoV, releasing its RNA for subsequent capture. However, we have observed that the BCoV vaccine used as a process control is subject to potential degradation during storage and handling and potential incomplete lysis during heat inactivation, possibly explaining the large variance in BCoV recovery with the 4S method. Recovery of PMMoV by 4S was also higher with heat pasteurization (twofold increase in recovery), but ultrafiltration was more effective in enriching PMMoV (1.6-fold higher than using the 4S-column method with heat pasteurization). Here, ultrafiltration may be effective in concentrating intact virus that is able to persist in wastewater, which is consistent with previous reports on PMMoV.^{24,25} Although we did not directly assess the state of SARS-CoV-2 in wastewater, these results may suggest that a fraction of SARS-CoV-2 RNA in the analyzed wastewater was not bound to viral particles but was present as free or ribonucleoprotein-bound RNA. This possibility is consistent with reports indicating reduced viability of SARS-CoV-2 and related coronaviruses spiked into wastewater, as well as preliminary reports demonstrating that wastewater SARS-CoV-2 genomes are predominantly decapsidated.^{26,27} Given that the 4S method is designed to lyse and extract wastewater RNAs without requiring the enrichment of viral particles, we also investigated whether the 4S method could recover human RNAs present in wastewater. Using the 4S method, we were able to recover and detect human ribosomal subunit RNA (18S rRNA) in wastewater influent (Supporting Information Figure S1A). 18S rRNA recovery was enhanced 2.5-fold by heat pasteurization, suggesting the lysis of human cells or 18S rRNA bound to ribonucleoprotein complexes present in wastewater (Supporting Information Figure S1A). Therefore, the 4S method enabled the recovery and detection of human RNA, another potential indicator of wastewater fecal concentration, which could allow direct normalization of SARS-CoV-2 RNA quantity to human RNA content of wastewater. As heat pasteurization did not affect 4S recovery

of SARS-CoV-2 and improved the recovery of PMMoV, BCoV, and 18S rRNA, we recommend integrating this pathogen-inactivation step to increase the safety of processing wastewater samples.

We sought to adapt the 4S strategy to employ silica powder for RNA capture rather than silica columns to circumvent reliance on commercially manufactured silica columns. In this approach, we added a slurry of silicon dioxide particles to lysed wastewater and used centrifugation to separate particle-bound RNA from the wastewater matrix, an approach we named “4S-Milk-of-Silica”. We observed that the 4S-Milk-of-Silica method recovered equivalent SARS-CoV-2 and PMMoV signals to the 4S method using a silica column (Supporting Information Figure S1B). Thus, the 4S-Milk-of-Silica method presents an even more cost-effective (~\$8 per sample vs ~\$13 per sample, using the 4S-column extraction method, Supporting Information Table S6) and accessible method to extract wastewater RNA without reliance on commercially manufactured silica columns and a vacuum manifold. However, the “Milk-of-Silica” version of the 4S protocol requires an isopropanol precipitation RNA concentration step, lengthening the protocol time. Therefore, we recommend using the 4S-column method to enable faster sample processing, while “4S-Milk-of-Silica” presents an alternate protocol for use in resource-limited settings.

Wastewater-Based Epidemiology Via the 4S Method.

WBE can provide an assessment of different areas’ relative COVID-19 infection prevalence, so we assessed whether the 4S-column extraction method could detect differential SARS-CoV-2 RNA levels in wastewaters derived from different subsections of a collection system. We surveyed three wastewater influent interceptors serving North and West Berkeley and El Cerrito (N), East Berkeley/Berkeley Hills (A), and Oakland (S) (interceptor area coverage shown in Supporting Information Figure S2A). These interceptors served areas exhibiting differential incidence of clinically confirmed COVID-19 cases, ranging from three (A interceptor) to 68 (S interceptor) reported cases per day within the week of our sampling (Figure S2A). To compare clinical COVID-19 clinical case data and wastewater SARS-CoV-2 concentration, we normalized the clinical case data by population, and we normalized the SARS-CoV-2 quantity by

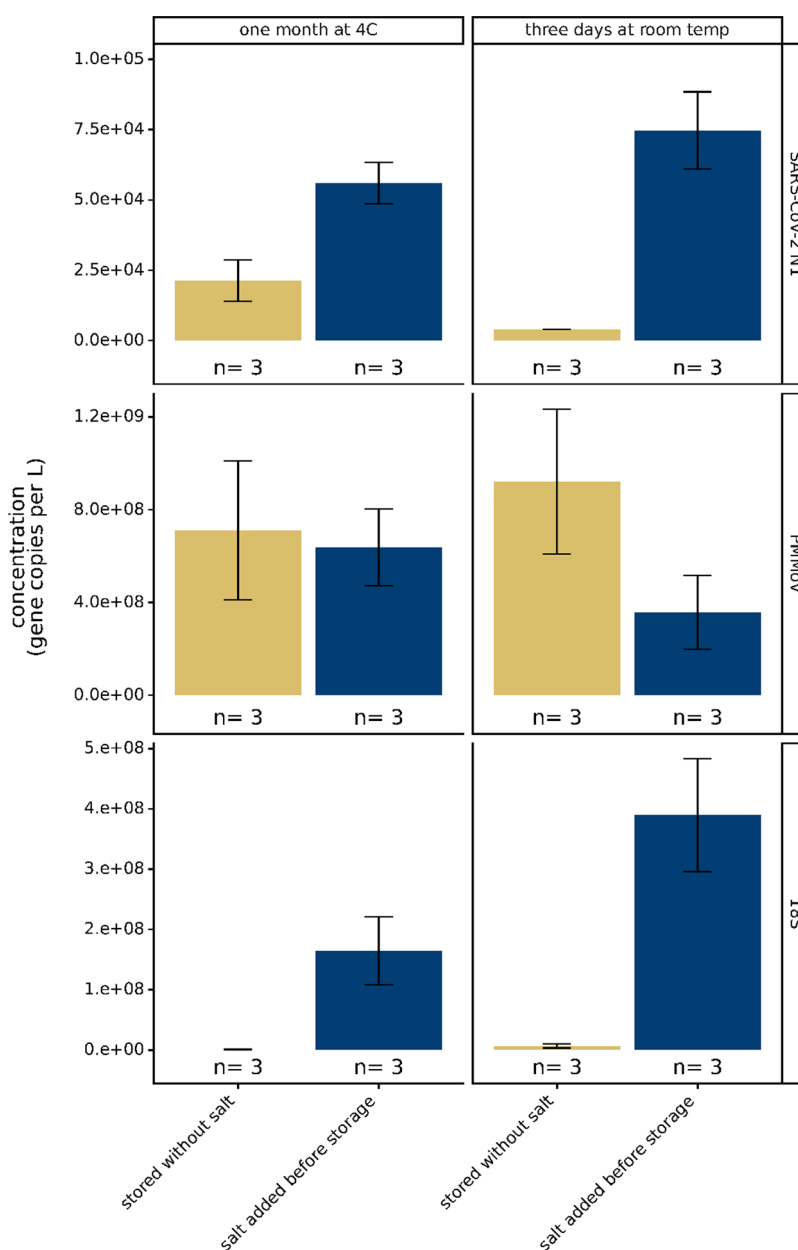


Figure 3. Effect of lysis salt addition prior to wastewater storage on SARS-CoV-2 N1, PMMoV, and 18S rRNA assay signals. “n” represents the number of storage and extraction biological replicates per condition. Bars are plotted at the arithmetic mean of biological triplicates and error bars represent the variation associated with biological triplicates as quantified by the arithmetic standard deviation of the biological triplicates.

PMMoV abundance, to control for fecal concentration in the wastewater. Detected wastewater SARS-CoV-2 concentrations are likely dependent on wastewater fecal concentration, which in turn varies based on the number of individuals contributing to the wastewater, wastewater flow rates, and water utilization. Future work into relating wastewater flow, solid content, and fecal concentration controls such as PMMoV may clarify true wastewater SARS-CoV-2 concentrations. Normalized wastewater SARS-CoV-2 signals followed per capita clinical cases per day in the three subwatersheds (Figure 2B). Raw SARS-CoV-2 and PMMoV abundance is available in Supporting Information Figure S2B. The normalized SARS-CoV-2 RNA concentration was highest in wastewater representing the S interceptor area, where the highest daily per capita new cases also occurred. Normalized SARS-CoV-2 RNA concentrations in wastewaters representing the N interceptor area were only

2.3-fold lower than those of S interceptor wastewaters, despite 11.6-fold fewer per capita daily cases being reported in the A interceptor area during the week of our sample collection. One possible reason for this difference could be the presence of undiagnosed infections in the N interceptor service area in which case wastewater SARS-CoV-2 RNA concentrations may provide a more accurate view of the relative COVID-19 infection prevalence in the week prior to sampling. Alternatively, the variability associated with wastewater measurements may be too large to detect differences of this magnitude.^{9,13} Ongoing research seeks to better quantify the measurement variability in wastewater samples over temporal and spatial scales. We emphasize that SARS-CoV-2 RNA levels were quantifiable in the A subwatershed despite only 18 cases being reported in an estimated population of 90,000 during the weeklong period of our sampling. This result implies that the

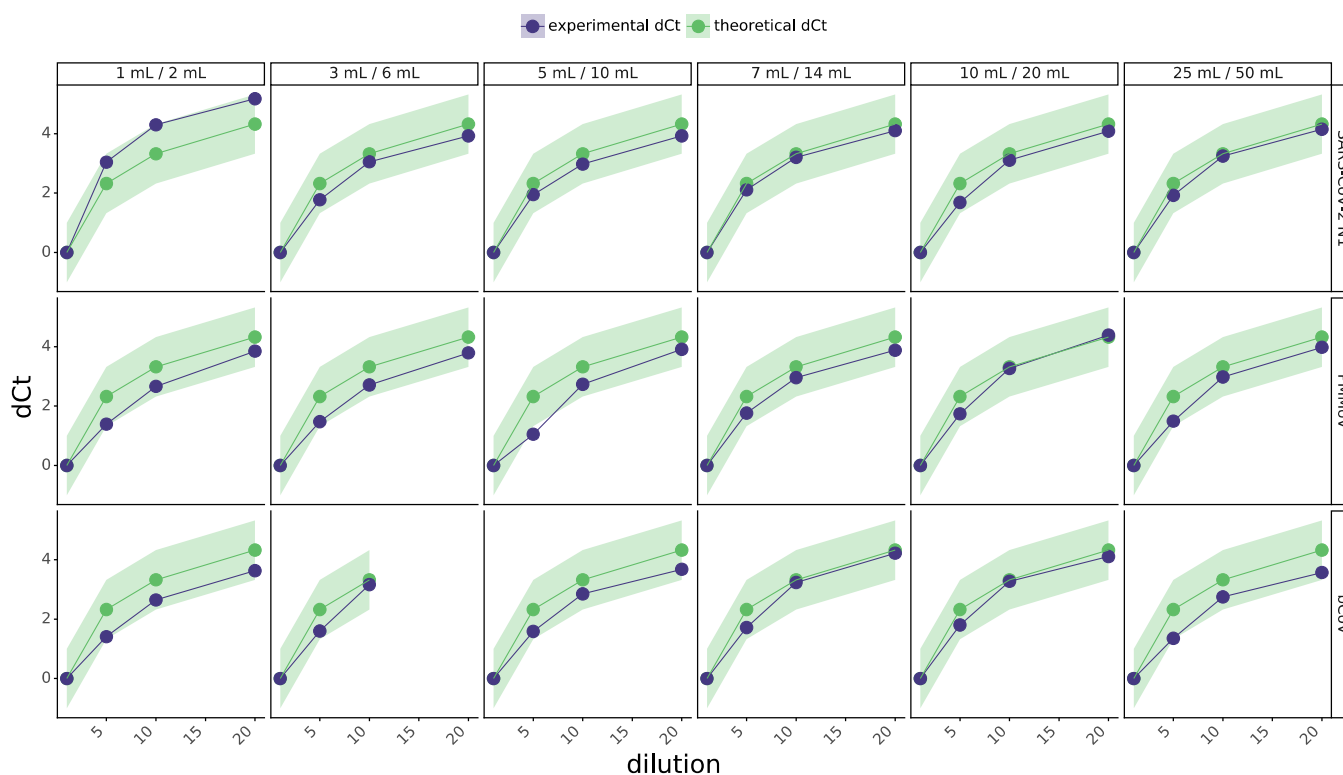


Figure 4. Assessment of RT-qPCR assay inhibition of the SARS-CoV-2 N1, PMMoV and BCoV assays via the “spike and dilute” method for different volumes of 4S-WB1 and 4S-WB2 (volumes reported at the top of each panel). Sample dilutions shown are 1 ×, 5 ×, 10 ×, and 20 ×. The green line with circular points represents theoretically expected increase in Ct due to sample dilution, and the blue line with triangular points indicates actual increase in Ct with sample dilution. The green band indicates +/− 1 Ct tolerance range around the expected Ct values, due to variability. An increase in the measured Ct that is lower than the expected increase was interpreted as inhibition. The RNA sample dilution factor is indicated on the x-axis.

4S method is highly sensitive and can be used to monitor areas with low COVID-19 prevalence.

Wastewater RNA Preservation and Purification Via the 4S Method. Wastewater contains many contaminants with the potential to degrade nucleic acids, and it has been previously observed that SARS-CoV-2 RNA in wastewater is degraded during storage.^{26,28,29} Viral detection relying on wastewater RNA extraction methods that concentrate intact viruses may be strongly affected by variable amounts of virus and viral RNA degradation in wastewater. Therefore, we sought to assess whether EDTA and sodium chloride, added to wastewater in the 4S method to promote lysis, could dually act to preserve RNA in wastewater. Upon receipt of each wastewater sample, we added NaCl to a final concentration of 4 M, added EDTA to a final concentration of 1 mM, and stored the samples either at 4 °C for a month or three days at room temperature (20 °C). We observed that salt and EDTA addition prior to storage improved the SARS-CoV-2 N1 assay signal after storage at both 4 °C for one month (2.6-fold higher signal when stored with salt and EDTA) or at 20 °C for three days (22-fold higher signal when stored with salt and EDTA) (Figure 3). Interestingly, the PMMoV assay signal remained similar throughout storage with or without salt, implying that PMMoV remains resistant to RNAses in the wastewater matrix. This observation corroborates previous reports indicating the persistence of PMMoV in sea and river water.^{24,25} As with the SARS-CoV-2 N1 signal, we observed that salt and EDTA addition preserved the human 18S rRNA signal at 4 °C for one month (126-fold higher) or at 20 °C for three days (56-fold higher) (Figure 3). These results may suggest that a portion of

SARS-CoV-2 in wastewater has been lysed, rendering its RNA more susceptible to degradation, while a greater portion of PMMoV may remain encapsidated, protecting its RNA from degradation. The nonenveloped enteric Coxsackievirus B5 was also recently reported to be more stable in wastewater than SARS-CoV-2.²⁷ Overall, the lysis salts added to wastewater as part of the normal 4S method workflow conveniently preserved wastewater RNAs and may mitigate degradation-mediated variation in SARS-CoV-2 and fecal concentration controls caused by RNA degradation during shipping and storage. However, we recommend extracting RNA from wastewater as soon as possible after sampling to ensure maximal RNA integrity.

Given the impact of RNA degradation on the SARS-CoV-2 N1 assay signal during wastewater storage, we investigated whether the bulk RNA yield could approximate the fecal load. However, the bulk RNA yield per mL of wastewater input correlated poorly with SARS-CoV-2 and PMMoV detection (Supporting Information Figure S3A), suggesting that the bulk of wastewater RNA is not contributed by fecal inputs. We also observed that extracting nucleic acids from increasing volumes of wastewater (up to 400 mL) did not strongly increase the total RNA yield per extraction past 100 mL of wastewater sample input, implying potential saturation of the RNA capture matrix (Supporting Information Figure S3B). From these experiments, we conclude that the RT-qPCR detection of human fecal concentration indicators such as PMMoV and human 18S rRNA, the latter of which is preserved during storage similarly to SARS-CoV-2, are suitable estimators of wastewater fecal concentration. Lastly, we observed that the 4S

method enriched up to 8 μg of DNA per 100 mL of wastewater, suggesting that the 4S method could be employed for future wastewater surveillance of DNA-based pathogens and DNA-sequencing-based wastewater surveys (Supporting Information Figure S3C).

Wastewater samples contain many contaminants that have previously been reported to inhibit RT-qPCR reactions.³⁰ Therefore, we sought to assess whether the 4S method could generate purified RNA free of RT-qPCR contaminants by employing the “spike and dilute” method to assess PCR inhibition.³¹ Here, we spiked purified wastewater RNA with a synthetic RNA standard and sequentially diluted the sample and observed whether SARS-CoV-2 N1, PMMoV, and BCoV detection followed corresponding sample dilutions, indicating an absence of inhibition. We assessed the impact of a range (1–50 mL) of wash buffer volumes during RNA extraction on PCR inhibition and SARS-CoV-2 N1, PMMoV, and BCoV assay signals to identify the optimal wash buffer volume for RNA purity and recovery. There was no evidence of inhibition for the SARS-CoV-2 N1 assay using the 4S procedure with any wash buffer volume, and slight inhibition of the PMMoV assay when using 5 mL of 4S-Wash buffer #1 (4S-WB1) and 10 mL of 4S-Wash buffer #2 (4S-WB2) (Figure 4). To limit ethanol waste generation, we therefore recommend using at least 7 mL of 4S-WB1 and 14 mL of 4S-WB2 to yield inhibitor-free RNA.

Next, we assessed potential assay signal loss due to excess washing of the silica columns. Here, we observed highest SARS-CoV-2, PMMoV, and BCoV assay signals using 3 mL of 4S-WB1 and 6 mL of Wash 4S-WB2, with no trend toward loss in SARS-CoV-2 and PMMoV signals up until 25 mL of 4S-WB1 and 50 mL of 4S-WB2, whereas we noticed a trend toward BCoV signal loss after 3 mL of 4S-WB1 and 6 mL of 4S-WB2 (Supporting Information Figure S4). Using too little wash buffer may not sufficiently wash away lysis salts and contaminants from the silica matrix, reducing RNA recovery and increasing inhibition, whereas too much wash buffer may partially elute bound RNA, decreasing the RNA yield. Therefore, we recommend using 7–10 mL of 4S-WB1 and 14–20 mL of 4S-WB2 to extract PCR inhibitor-free RNA while maximizing target RNA recovery.

The results presented here are representative of only three wastewater sources which may differ in composition from wastewater collected at other times and from other locations. Different wastewaters may contain different types and quantities of PCR inhibitors, so we recommend assessing PCR inhibition in all sample types, and if necessary, adjusting the wash buffer volumes to effectively remove inhibitors from the purified RNA. Different wastewater samples may also contain varying biological and chemical species influencing RNA stability, potentially impacting the RNA preservation documented here by the 4S method. Furthermore, the 4S method may be less effective in capturing the nucleic acids from wastewater viruses or other microorganisms resistant to the sodium chloride and heat-based lysis evaluated here.

Overall, we demonstrate that the 4S method enabled efficient extraction of SARS-CoV-2, PMMoV, BCoV, and human 18S rRNA. Combined with RT-qPCR, the 4S method allowed monitoring of relative COVID-19 infection prevalence with high sensitivity. These results are consistent with those of a recent interlaboratory comparison of 36 different wastewater SARS-CoV-2 RNA detection methods. In this comparison, the concentration of SARS-CoV-2 measured with the 4S method, identified as “1S.2H”, was one of the highest reported (direct

measurement, without correcting for recovery efficiency) and the recovery efficiency of a spiked-in OC43 virus efficiency control was the highest reported, among all methods.³² The 4S method also preserved RNA in wastewater, was compatible with heat pasteurization, and yielded purified RNA free of PCR inhibitors. Given the high efficiency, low cost, and same-day assessment of wastewater SARS-CoV-2 and fecal concentration controls, the 4S method presents an affordable and accessible method for implementing wastewater-based epidemiology for SARS-CoV-2. This method also appears promising for the application of WBE for other RNA- and DNA-based pathogens and facilitating research on the wastewater microbial community more broadly.

■ ASSOCIATED CONTENT

Supporting Information

The Supporting Information is available free of charge at <https://pubs.acs.org/doi/10.1021/acs.est.0c08129>.

The supporting information details supplementary figures, methods, and data analysis.

Impact of heat inactivation on 4S-column recovery of 18 s rRNA, “Milk-of-Silica” silicon dioxide RNA extraction strategy performance; wastewater interceptor coverage, individual A, N, and S interceptor SARS-CoV-2 and PMMoV concentration measurements associated with Figure 2; relation of extracted RNA concentration to SARS-CoV-2 N1 and PMMoV assay signals, relationship between the wastewater input and RNA yield using the 4S-column, Milk-of-Silica, ultrafiltration and ultrafiltration and solids extraction methods, and relationship between the wastewater input volume and DNA yield; impact of wash buffer volume use on SARS-CoV-2 N1, PMMoV, and BCoV recovery; RT-qPCR reaction conditions (Table S1); RT-qPCR thermocycling parameters (Table S2); qPCR assay information for the SARS-CoV-2 nucleocapsid N gene (N1), the bovine coronavirus transmembrane protein gene (bCoV), the pepper mild mottle virus coat protein gene (PMMoV), and human 18S ribosomal rRNA (18S) (Table S3); RT-qPCR validation information (Table S4); evidence for LoD/LoQ (Table S5); reagent cost of the 4S method using a silica column or silicon dioxide particulate (Table S6) MIQE guideline essential information checklist (Table S7); and nucleic acid quantification, target RNA detection via RT-qPCR, and data analysis methods (PDF)

■ AUTHOR INFORMATION

Corresponding Author

Kara L. Nelson – Department of Civil and Environmental Engineering, University of California, Berkeley, California 94720-1710, United States; Innovative Genomics Institute, Berkeley, California 94704, United States; orcid.org/0000-0001-8899-2662; Email: karanelson@berkeley.edu

Authors

Oscar N. Whitney – Department of Molecular and Cell Biology, University of California, Berkeley, California 94720-1710, United States; orcid.org/0000-0002-4858-2615

Lauren C. Kennedy – Department of Civil and Environmental Engineering, University of California,

Berkeley, California 94720-1710, United States;

orcid.org/0000-0002-4451-2361

Vinson B. Fan – Department of Molecular and Cell Biology, University of California, Berkeley, California 94720-1710, United States

Adrian Hinkle – Department of Civil and Environmental Engineering, University of California, Berkeley, California 94720-1710, United States

Rose Kantor – Department of Civil and Environmental Engineering, University of California, Berkeley, California 94720-1710, United States; orcid.org/0000-0002-5402-8979

Hannah Greenwald – Department of Civil and Environmental Engineering, University of California, Berkeley, California 94720-1710, United States

Alexander Crits-Christoph – Department of Plant and Microbial Biology, University of California, Berkeley, California 94720-1710, United States; Innovative Genomics Institute, Berkeley, California 94704, United States

Basem Al-Shayeb – Department of Plant and Microbial Biology, University of California, Berkeley, California 94720-1710, United States; Innovative Genomics Institute, Berkeley, California 94704, United States

Mira Chaplin – Department of Civil and Environmental Engineering, University of California, Berkeley, California 94720-1710, United States

Anna C. Maurer – Department of Molecular and Cell Biology, University of California, Berkeley, California 94720-1710, United States

Robert Tjian – Department of Molecular and Cell Biology, University of California, Berkeley, California 94720-1710, United States; The Howard Hughes Medical Institute, University of California Berkeley, Berkeley, California 94720, United States

Complete contact information is available at:
<https://pubs.acs.org/10.1021/acs.est.0c08129>

Funding

O.N.W. is supported by the NIH training program grant T32GM007232. We gratefully acknowledge funding from the Howard Hughes Medical Institute (grant CC34430 to R.T.) and from rapid response grants from the Center for Information Technology Research in the Interest of Society (CITRIS), the Catena Foundation and the Innovative Genomics Institute (IGI) at UC Berkeley to K.L.N.

Notes

The authors declare no competing financial interest.

ACKNOWLEDGMENTS

We thank all members of the Nelson laboratory and UC Berkeley COVID-WEB pop-up lab for their contributions, reading, insights and helpful discussions of this paper. We also thank all members of the Tjian and Darzacq lab for their support designing and carrying out molecular assays and experiments. We thank the East Bay Municipal Utility District for sample collection.

REFERENCES

(1) Bivins, A.; North, D.; Ahmad, A.; Ahmed, W.; Alm, E.; Been, F.; Bhattacharya, P.; Bijlsma, L.; Boehm, A. B.; Brown, J.; Buttiglieri, G.; Calabro, V.; Carducci, A.; Castiglioni, S.; Cetecioglu Guro, Z.; Chakraborty, S.; Costa, F.; Curcio, S.; de los Reyes, F. L.; Delgado

Vela, J.; Farkas, K.; Fernandez-Casi, X.; Gerba, C.; Gerrity, D.; Girones, R.; Gonzalez, R.; Haramoto, E.; Harris, A.; Holden, P. A.; Islam, M. T.; Jones, D. L.; Kasprzyk-Hordern, B.; Kitajima, M.; Kotlarz, N.; Kumar, M.; Kuroda, K.; La Rosa, G.; Malpei, F.; Mautus, M.; McLellan, S. L.; Medema, G.; Meschke, J. S.; Mueller, J.; Newton, R. J.; Nilsson, D.; Noble, R. T.; van Nuijs, A.; Peccia, J.; Perkins, T. A.; Pickering, A. J.; Rose, J.; Sanchez, G.; Smith, A.; Stadler, L.; Stauber, C.; Thomas, K.; van der Voorn, T.; Wigginton, K.; Zhu, K.; Bibby, K. Wastewater-Based Epidemiology: Global Collaborative to Maximize Contributions in the Fight Against COVID-19. *Environ. Sci. Technol.* **2020**, *54*, 7754–7757.

(2) Zhou, N. A.; Fagnant-Sperati, C. S.; Komen, E.; Mwangi, B.; Mukubi, J.; Nyangao, J.; Hassan, J.; Chepkurui, A.; Maina, C.; van Zyl, W. B.; Matsapola, P. N.; Wolfaardt, M.; Ngwana, F. B.; Jeffries-Miles, S.; Coulliette-Salmond, A.; Peñaranda, S.; Shirai, J. H.; Kossik, A. L.; Beck, N. K.; Wilmouth, R.; Boyle, D. S.; Burns, C. C.; Taylor, M. B.; Borus, P.; Meschke, J. S. Feasibility of the Bag-Mediated Filtration System for Environmental Surveillance of Poliovirus in Kenya. *Food Environ. Virol.* **2020**, *12*, 35–47.

(3) Kazama, S.; Miura, T.; Masago, Y.; Konta, Y.; Tohma, K.; Manaka, T.; Liu, X.; Nakayama, D.; Tanno, T.; Saito, M.; Oshitani, H.; Omura, T. Environmental Surveillance of Norovirus Genogroups I and II for Sensitive Detection of Epidemic Variants. *Appl. Environ. Microbiol.* **2017**, *83*, e03406–e03416.

(4) Kaliner, E.; Kopel, E.; Anis, E.; Mendelson, E.; Moran-Gilad, J.; Shulman, L. M.; Singer, S. R.; Manor, Y.; Somekh, E.; Rishpon, S.; Leventhal, A.; Rubin, L.; Tasher, D.; Honovich, M.; Moerman, L.; Shohat, T.; Bassal, R.; Sofer, D.; Gdalevich, M.; Lev, B.; Gamzu, R.; Grotto, I. The Israeli Public Health Response to Wild Poliovirus Importation. *Lancet Infect. Dis.* **2015**, *15*, 1236–1242.

(5) Hata, A.; Honda, R. Potential Sensitivity of Wastewater Monitoring for SARS-CoV-2: Comparison with Norovirus Cases. *Environ. Sci. Technol.* **2020**, *54*, 6451–6452.

(6) Li, R.; Pei, S.; Chen, B.; Song, Y.; Zhang, T.; Yang, W.; Shaman, J. Substantial Undocumented Infection Facilitates the Rapid Dissemination of Novel Coronavirus (SARS-CoV-2). *Science* **2020**, *368*, 489–493.

(7) Wu, Y.; Guo, C.; Tang, L.; Hong, Z.; Zhou, J.; Dong, X.; Yin, H.; Xiao, Q.; Tang, Y.; Qu, X.; Kuang, L.; Fang, X.; Mishra, N.; Lu, J.; Shan, H.; Jiang, G.; Huang, X. Prolonged Presence of SARS-CoV-2 Viral RNA in Faecal Samples. *Lancet Gastroenterol. Hepatol.* **2020**, *5*, 434–435.

(8) Holshue, M. L.; DeBolt, C.; Lindquist, S.; Lofy, K. H.; Wiesman, J.; Bruce, H.; Spitters, C.; Ericson, K.; Wilkerson, S.; Tural, A.; Diaz, G.; Cohn, A.; Fox, L.; Patel, A.; Gerber, S. I.; Kim, L.; Tong, S.; Lu, X.; Lindstrom, S.; Pallansch, M. A.; Weldon, W. C.; Biggs, H. M.; Uyeki, T. M.; Pillai, S. K. First Case of 2019 Novel Coronavirus in the United States. *N. Engl. J. Med.* **2020**, *382*, 929–936.

(9) Peccia, J.; Zulli, A.; Brackney, D. E.; Grubaugh, N. D.; Kaplan, E. H.; Casanovas-Massana, A.; Ko, A. I.; Malik, A. A.; Wang, D.; Wang, M.; Warren, J. L.; Weinberger, D. M.; Arnold, W.; Omer, S. B. Measurement of SARS-CoV-2 RNA in Wastewater Tracks Community Infection Dynamics. *Nat. Biotechnol.* **2020**, *38*, 1164–1167.

(10) Ahmed, W.; Angel, N.; Edson, J.; Bibby, K.; Bivins, A.; O'Brien, J. W.; Choi, P. M.; Kitajima, M.; Simpson, S. L.; Li, J.; Tschärke, B.; Verhagen, R.; Smith, W. J. M.; Zaugg, J.; Dierens, L.; Hugenholtz, P.; Thomas, K. V.; Mueller, J. F. First Confirmed Detection of SARS-CoV-2 in Untreated Wastewater in Australia: A Proof of Concept for the Wastewater Surveillance of COVID-19 in the Community. *Sci. Total Environ.* **2020**, *728*, 138764.

(11) Medema, G.; Heijnen, L.; Elsinga, G.; Italiaander, R.; Brouwer, A. Presence of SARS-Coronavirus-2 RNA in Sewage and Correlation with Reported COVID-19 Prevalence in the Early Stage of the Epidemic in The Netherlands. *Environ. Sci. Technol. Lett.* **2020**, *7*, 511–516.

(12) Crits-Christoph, A.; Kantor, R. S.; Olm, M. R.; Whitney, O. N.; Al-Shayeb, B.; Lou, Y. C.; Flamholz, A.; Kennedy, L. C.; Greenwald, H.; Hinkle, A.; Hetzel, J.; Spitzer, S.; Koble, J.; Tan, A.; Hyde, F.; Schroth, G.; Kuersten, S.; Banfield, J. F.; Nelson, K. L. *Genome*

Sequencing of Sewage Detects Regionally Prevalent SARS-CoV-2 Variants. medRxiv 2020, DOI: 10.1101/2020.09.13.20193805.

(13) Kitajima, M.; Ahmed, W.; Bibby, K.; Carducci, A.; Gerba, C. P.; Hamilton, K. A.; Haramoto, E.; Rose, J. B. SARS-CoV-2 in Wastewater: State of the Knowledge and Research Needs. *Sci. Total Environ.* **2020**, *739*, No. 139076.

(14) La Rosa, G.; Bonadonna, L.; Lucentini, L.; Kenmoe, S.; Suffredini, E. Coronavirus in Water Environments: Occurrence, Persistence and Concentration Methods - A Scoping Review. *Water Res.* **2020**, *179*, No. 115899.

(15) Lu, D.; Huang, Z.; Luo, J.; Zhang, X.; Sha, S. Primary Concentration – The Critical Step in Implementing the Wastewater Based Epidemiology for the COVID-19 Pandemic: A Mini-Review. *Sci. Total Environ.* **2020**, *747*, No. 141245.

(16) Satyanarayana, M. Shortage of RNA extraction kits hampers efforts to ramp up COVID-19 coronavirus testing <https://cen.acs.org/analytical-chemistry/diagnostics/Shortage-RNA-extraction-kits-hampers/98/web/2020/03> (accessed Nov 9, 2020).

(17) LaTurner, Z. W.; Zong, D. M.; Kalvapalle, P.; Gamas, K. R.; Terwilliger, A.; Crosby, T.; Ali, P.; Avadhanula, V.; Santos, H. H.; Weesner, K.; Hopkins, L.; Piedra, P. A.; Maresso, A. W.; Stadler, L. B. *Evaluating Recovery, Cost, and Throughput of Different Concentration Methods for SARS-CoV-2 Wastewater-Based Epidemiology.* medRxiv 2020, DOI: 10.1101/2020.11.27.20238980.

(18) CDC. *Coronavirus Disease 2019 (COVID-19)* <https://www.cdc.gov/coronavirus/2019-ncov/cases-updates/wastewater-surveillance/testing-methods.html> (accessed Nov 9, 2020).

(19) Kitajima, M.; Sassi, H. P.; Torrey, J. R. Pepper Mild Mottle Virus as a Water Quality Indicator. *Npj Clean Water* **2018**, *1*, 1–9.

(20) Whitney, O. *Direct Wastewater RNA Capture and Purification via the "Sewage, Salt, Silica and SARS-CoV-2 (4S)" Method.* 2020. DOI: 10.17504/protocols.io.biwekfb.

(21) Whitney, O. *Direct Wastewater RNA Extraction via the "Milk of Silica (MoS)" Method - A Companion Method to "Sewage, Salt, Silica and SARS-CoV-2 (4S)" Method.* 2020. DOI: 10.17504/protocols.io.biwfkfbn.

(22) Graham, T. G. W.; Dugast-Darzacq, C.; Dailey, G. M.; Nguyenla, X. H.; Van Dis, E.; Esbin, M. N.; Abidi, A.; Stanley, S. A.; Darzacq, X.; Tjian, R., Inexpensive, Versatile and Open-Source Methods for SARS-CoV-2 Detection. preprint . *Infectious Diseases (except HIV/AIDS)*. 2020. DOI: 10.1101/2020.09.16.20193466.

(23) Wang, X.-W.; Li, J.-S.; Guo, T.-K.; Zhen, B.; Kong, Q.-X.; Yi, B.; Li, Z.; Song, N.; Jin, M.; Xiao, W.-J.; Zhu, X.-M.; Gu, C.-Q.; Yin, J.; Wei, W.; Yao, W.; Liu, C.; Li, J.-F.; Ou, G.-R.; Wang, M.-N.; Fang, T.-Y.; Wang, G.-J.; Qiu, Y.-H.; Wu, H.-H.; Chao, F.-H.; Li, J.-W. Concentration and Detection of SARS Coronavirus in Sewage from Xiao Tang Shan Hospital and the 309th Hospital. *J. Virol. Methods* **2005**, *128*, 156–161.

(24) Hamza, I. A.; Jurzik, L.; Überla, K.; Wilhelm, M. Evaluation of Pepper Mild Mottle Virus, Human Picobirnavirus and Torque Teno Virus as Indicators of Fecal Contamination in River Water. *Water Res.* **2011**, *45*, 1358–1368.

(25) Symonds, E. M.; Rosario, K.; Breitbart, M. Pepper Mild Mottle Virus: Agricultural Menace Turned Effective Tool for Microbial Water Quality Monitoring and Assessing (Waste)Water Treatment Technologies. *PLoS Pathog.* **2019**, *15*, No. e1007639.

(26) Bivins, A.; Greaves, J.; Fischer, R.; Yinda, K. C.; Ahmed, W.; Kitajima, M.; Munster, V. J.; Bibby, K. Persistence of SARS-CoV-2 in Water and Wastewater. *Environ. Sci. Technol. Lett.* **2020**, *7*, 937–942.

(27) Wurtzer, S.; Waldman, P.; Ferrier-Rembert, A.; Frenois-Veyrat, G.; Mouchel, J.; Boni, M.; Maday, Y.; Consortium, O.; Marechal, V.; Moulin, L. *Several Forms of SARS-CoV-2 RNA Can Be Detected in Wastewaters : Implication for Wastewater-Based Epidemiology and Risk Assessment.* medRxiv 2020, DOI: 10.1101/2020.12.19.20248508.

(28) Ahmed, W.; Bertsch, P. M.; Bibby, K.; Haramoto, E.; Hewitt, J.; Huygens, F.; Gyawali, P.; Korajkic, A.; Riddell, S.; Sherchan, S. P.; Simpson, S. L.; Sirikanchana, K.; Symonds, E. M.; Verhagen, R.; Vasan, S. S.; Kitajima, M.; Bivins, A. Decay of SARS-CoV-2 and Surrogate Murine Hepatitis Virus RNA in Untreated Wastewater to

Inform Application in Wastewater-Based Epidemiology. *Environ. Res.* **2020**, *191*, No. 110092.

(29) Michael-Kordatou, I.; Karaolia, P.; Fatta-Kassinos, D. Sewage Analysis as a Tool for the COVID-19 Pandemic Response and Management: The Urgent Need for Optimised Protocols for SARS-CoV-2 Detection and Quantification. *J. Environ. Chem. Eng.* **2020**, *8*, No. 104306.

(30) Schrader, C.; Schielke, A.; Ellerbroek, L.; John, R. PCR Inhibitors – Occurrence, Properties and Removal. *J. Appl. Microbiol.* **2012**, *113*, 1014–1026.

(31) Cao, Y.; Griffith, J. F.; Dorevitch, S.; Weisberg, S. B. Effectiveness of QPCR Permutations, Internal Controls and Dilution as Means for Minimizing the Impact of Inhibition While Measuring *Enterococcus* in Environmental Waters. *J. Appl. Microbiol.* **2012**, *113*, 66–75.

(32) Pecson, B. M.; Darby, E.; Haas, C. N.; Amha, Y.; Bartolo, M.; Danielson, R.; Dearborn, Y.; Giovanni, G. D.; Ferguson, C.; Fevig, S.; Gaddis, E.; Gray, D.; Lukasik, G.; Mull, B.; Olivas, L.; Olivieri, A.; Qu, Y.; Consortium, S.-C.-2 I *Reproducibility and Sensitivity of 36 Methods to Quantify the SARS-CoV-2 Genetic Signal in Raw Wastewater: Findings from an Interlaboratory Methods Evaluation in the U.S.* medRxiv 2020, DOI: 10.1101/2020.11.02.20221622.

Sewage, Salt, Silica and SARS-CoV-2 (4S): An economical kit-free method for direct capture of SARS-CoV-2 RNA from wastewater.

Oscar N. Whitney¹, Lauren C. Kennedy², Vinson B. Fan¹, Adrian Hinkle², Rose Kantor², Hannah Greenwald², Alexander Crits-Christoph^{3,4}, Basem Al-Shayeb^{3,4}, Mira Chaplin², Anna C. Maurer¹, Robert Tjian^{1,5}, Kara L. Nelson^{2,4†}

†Corresponding author: karanelson@berkeley.edu

¹Department of Molecular and Cell Biology, University of California, Berkeley, CA, USA

²Department of Civil and Environmental Engineering, University of California, Berkeley, CA, USA

³Department of Plant and Microbial Biology, University of California, Berkeley, CA, USA

⁴Innovative Genomics Institute, Berkeley, CA, 94704, USA

⁵The Howard Hughes Medical Institute, University of California Berkeley, Berkeley, California 94720, USA

Content summary: 19 pages, 4 figures and 7 tables.

Supporting Information

Supplementary Methods

Nucleic acid quantification

For all extraction methods, RNA and DNA yields were quantified using the Qubit 4 fluorometer high sensitivity RNA, broad range RNA and broad range DNA quantification assays, following manufacturer instructions. For part of the experiment shown in Supplementary Figure S3A, the solids pellets from slow centrifugation were resuspended in the ultrafiltrate concentrates and used as input for RNA extraction prior to nucleic acid quantification.

Target RNA detection via RT-qPCR

Quantification of target RNA species was performed using reverse transcription quantitative polymerase chain reaction (RT-qPCR) in technical triplicate with a QuantStudio 3 Real-Time PCR System (ThermoFisher Scientific). Each 20- μ L reaction included extracted RNA (5 μ L) and TaqMan Fast Virus 1-Step Master Mix (ThermoFisher Scientific), unless otherwise stated, as well as primers, probes, and RNase/DNase-free water (Table S1). This study employed four primer and probe sets (Table S3; Integrated DNA Technologies) targeting the SARS-CoV-2 nucleocapsid N gene (N1; 2019-nCoV CDC RUO kit), bovine coronavirus transmembrane protein gene (BCoV; custom DNA oligos), Pepper mild mottle virus coat protein gene (PMMoV; custom DNA oligos) and human 18S ribosomal rRNA (18S; custom DNA oligos).^{1,2} Assay thermocycling conditions are detailed in Table S2, and primer sequence information is in Table S3. Each plate included triplicate no template controls (NTCs) and RNA standards in 10-fold serial dilutions from different manufacturers: for the N1 Assay, synthetic SARS-CoV-2

RNA was used (Control 2- 102024, Twist Bioscience, San Francisco, CA); for bCoV and PMMoV, custom Ultramer RNA Oligonucleotides were used (Integrated DNA Technologies); and for 18S, RNA was in-vitro transcribed from an 18S target amplicon geneBlock (Integrated DNA Technologies) using the HiScribe T7 Quick High Yield RNA Synthesis Kit (New England Biolabs). Throughout all experiments, two no template controls amplified, but both were at least 8 Cq higher than that of the lowest point on the standard curve, and standard curve efficiencies ranged from 71% to 105%. Quality assessment data (including efficiencies and R² values by plate) are detailed in the supporting information (Table S4). Inhibition testing was completed once for each wash buffer condition for the N1, bCoV, and PMMoV assays following the spike and dilute method (Figure 4).³ A MIQE guideline checklist for this manuscript can be found in table S6.⁴

Data analysis

All associated code is available through Zenodo at DOI 10.5281/zenodo.4570691 and Github https://github.com/wastewaterlab/data_analysis_4S_manuscript/tree/V1.0. qPCR technical triplicate Cq values were determined through automatic thresholding on QuantStudio 3 Design and Analysis Software (v1.5.1). These values were imported into a custom data analysis pipeline in python (v3.6.9) which utilized key modules for manipulation (Pandas v1.1.2), calculations (NumPy v1.18.5 and SciPy v1.4.1), and visualizations (plotnine v0.6.0). First, for RT-qPCR technical triplicates, outlier identification and disposition were performed using the two-sided Grubbs test (with alpha = 0.05) in the scikit-posthocs module (v0.6.6; Table S5). After outlier detection and removal, the arithmetic mean of technical replicates was determined for samples and standards with two or more technical replicates. To adjust for fecal concentration, a normalized value was calculated by dividing the quantity (gc/L) of N1 by the associated

PMMoV quantity (gc/L) for comparisons with population COVID-19 case data.^{5,6} Linear regression was performed using plate-specific standard curves, unless otherwise stated, to determine associated quantity in gene copies per reaction in samples. Plates 35 and 38 did not have associated standard curves, thus the standard curve from plate 32 was used (all bCoV plates). Samples were considered below the limit of quantification if the Cq was higher than the Cq of the lowest quantity on the standard curve of the plate, or if the Cq was greater than 40. One hundred percent of replicates used in standard curves for 18S and PMMoV were detected. However, for N1 and bCoV, the limit of detection was set to be 20 and 1000 gene copies per reaction, respectively; the resulting percentage of detectable replicates was 89% (Table S5). Twelve samples were deemed below the limit of quantification or below the limit of detection; the limit of detection was used for these samples for plotting and data analysis. The quantity values were converted to gene copies per liter of wastewater for test group comparisons.

The geometric mean and geometric standard deviation (log scale plots) or the arithmetic mean and arithmetic standard deviation (linear plots) of biological replicates was determined, and all error bars in this manuscript are from biological replicates with number of replicates (n) shown on each plot. Normalized N1 to PMMoV values as well as gene copy per L data for all targets were not normally distributed, thus the statistical method used to assess results significance in Figure 2 was the Kruskal Wallis nonparametric test with paired Dunn's test of individual pairs.

To compare wastewater results with clinical data, publicly available new cases per day data from Alameda county⁷ and Contra Costa county⁸ were used (see also Zenodo and Github repository). To estimate new cases per day in each sub-sewershed, shape files of the A, N, and S sub-sewersheds (Figure S1) and of zip codes in California were overlaid in GeoPandas (v0.8.1). For Alameda county data, new cases per day in each sub-sewershed was estimated by weighting the

average new cases in each zip code by the overlap of the zip code with the interceptor. The N sub-sewershed is part of both Alameda and Contra Costa county. Thus, for N, Alameda county estimated new cases per day was added to the Contra Costa county estimate of new cases, which was estimated by weighting the average new cases by the area overlap of Contra Costa county with the N interceptor. New cases per capita was calculated by dividing the resulting new cases per day by the population in each sub-sewershed estimated by EBMUD (A: 90,000, N: 130,000, S: 465000).

All associated code is available through Zenodo at DOI 10.5281/zenodo.4570691 and Github https://github.com/wastewaterlab/data_analysis_4S_manuscript/tree/V1.0.

Supplementary figures

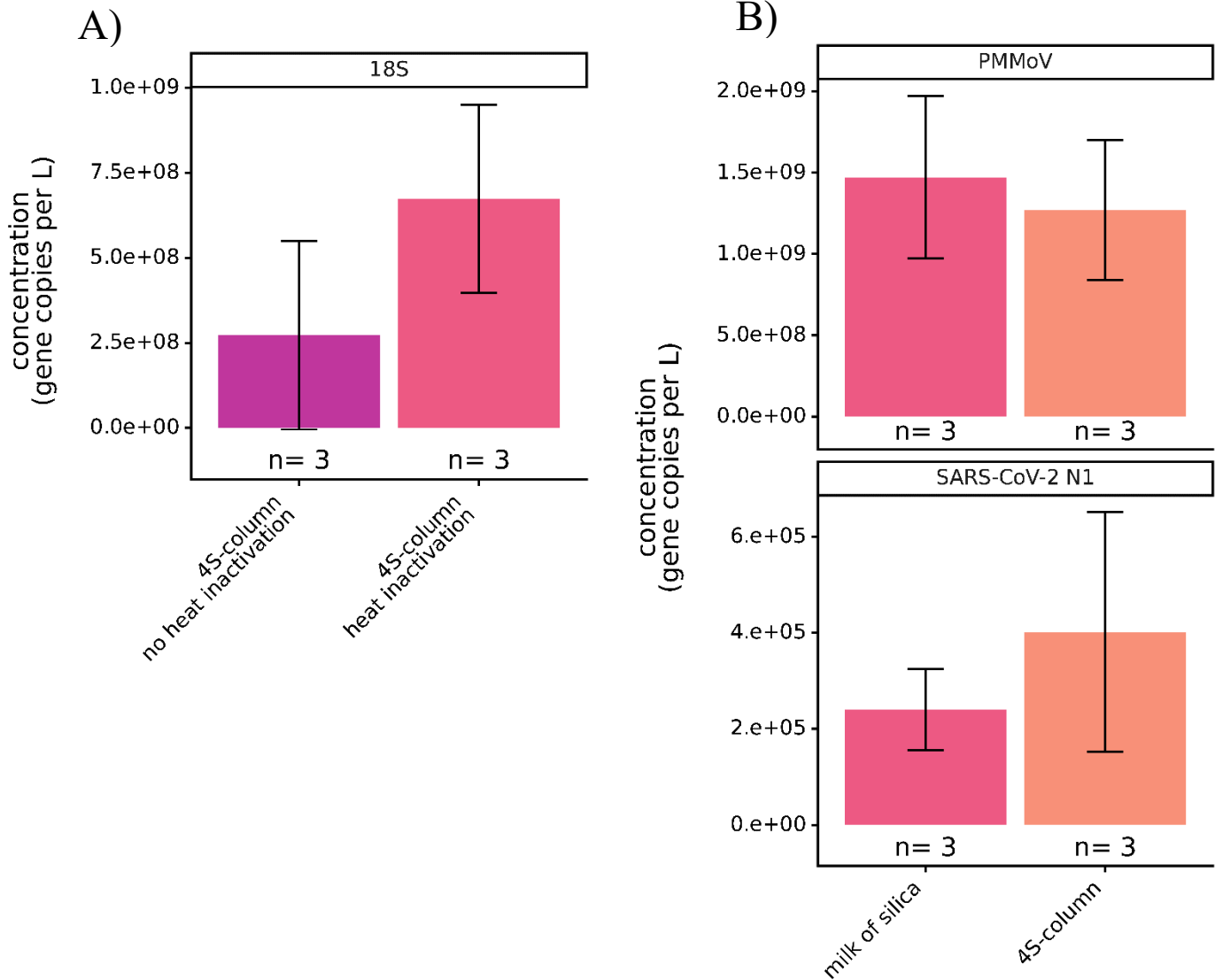


Figure 1. A) 18S rRNA assay signal of wastewater RNA purified via the 4S method, with and without heat inactivation. B) SARS-CoV-2 N1 assay and PMMoV assay signal of wastewater RNA purified via the 4S method using “Milk-of-Silica” silicon dioxide particulate (milk of silica) or silica-containing spin columns (4S-column). “n” represents the number of wastewater RNA extraction biological replicates per condition. Bars are plotted at the arithmetic mean of biological triplicates and error bars represent the variation associated with biological triplicates as quantified by the arithmetic standard deviation of the biological triplicates.

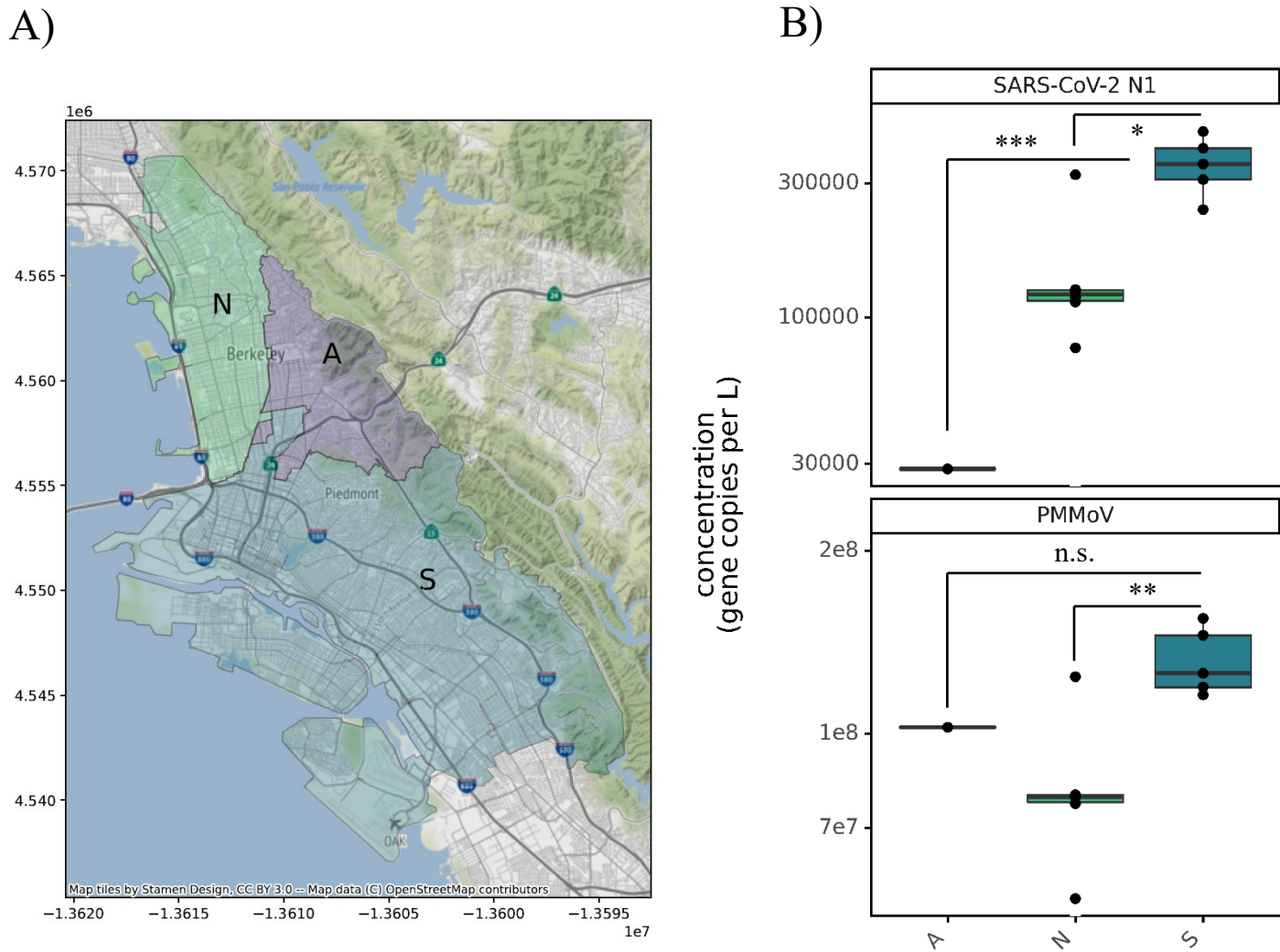
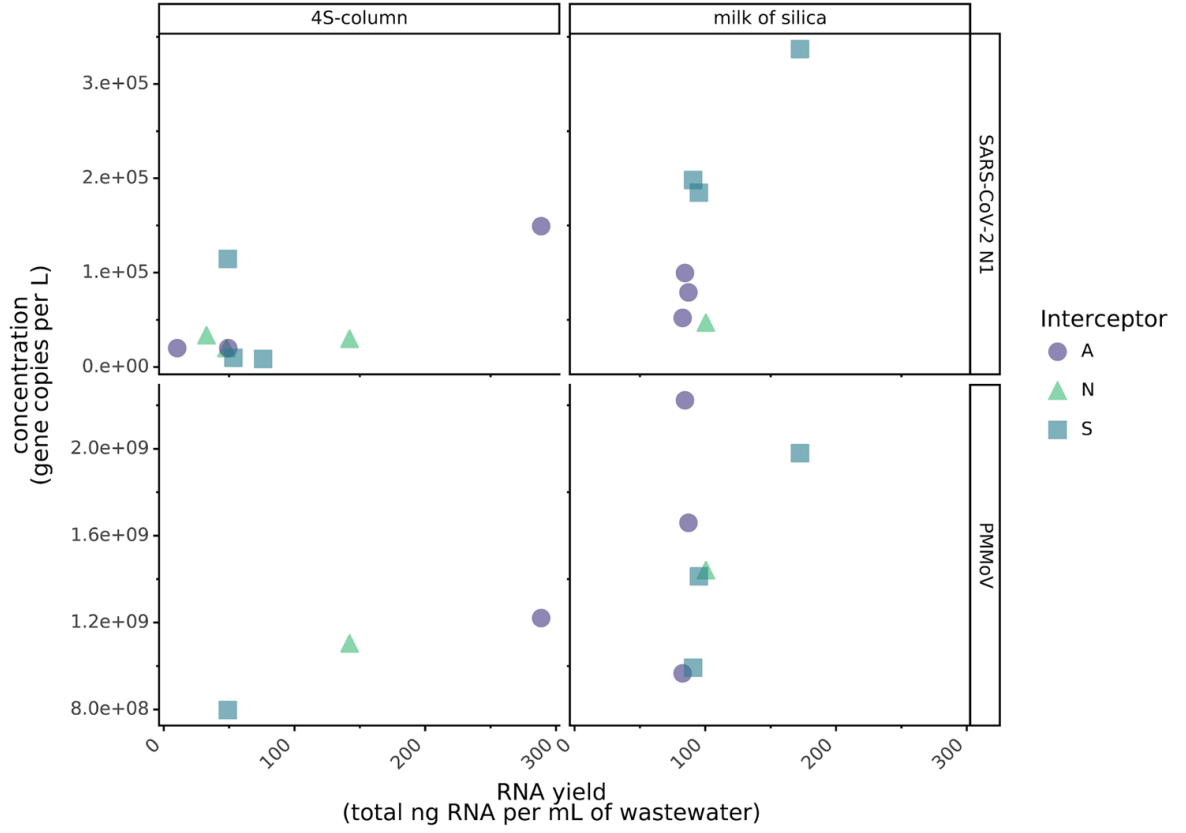
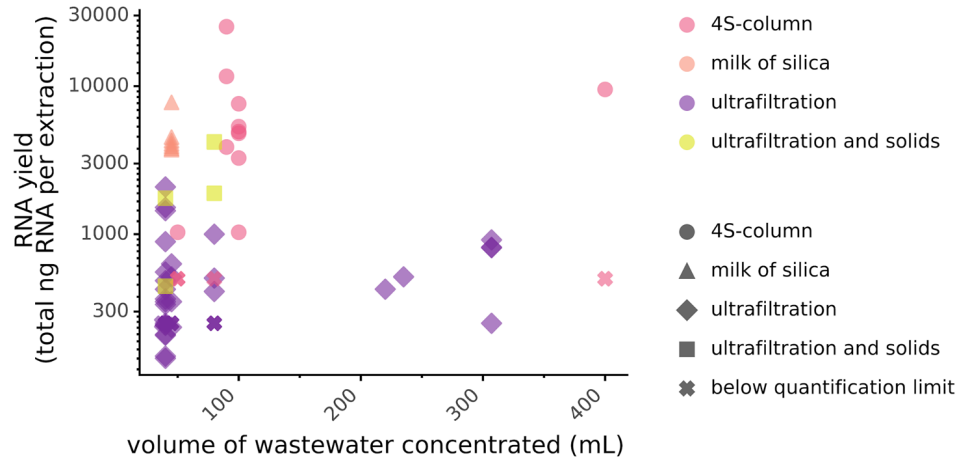


Figure S2. A) Sewersheds served by the East Bay Municipal Utility District N, A, and S interceptors. B) SARS-CoV-2 N1 assay and PMMoV assay signal of wastewater RNAs extracted from the A, N and S interceptors. “n” represents the number of wastewater RNA extraction biological replicates per assay. Kruskal-Wallis test followed by Dunn’s test was performed to determine significance, where $*=p<0.05$, $***=p<0.001$, n.s. = not significant.

A)



B)



C)

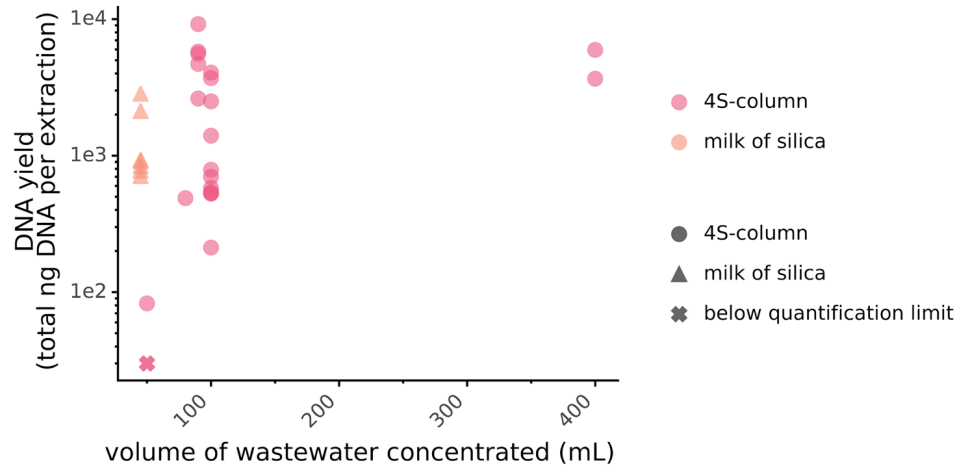


Figure S3. A) Relation of extracted RNA concentration to SARS-CoV-2 N1 and PMMoV assay signal reported as concentration in gene copies per liter, using the 4S-column or Milk-of silica method. X-axis represents RNA yield, defined as ng of RNA extracted per mL of wastewater input.

B) Relationship between wastewater input and RNA yield using 4 different methods, defined as total ng of RNA per extraction. Column (pink) represents the 4S method using a silica column, Milk of Silica (salmon) represents the 4S method using a silicon dioxide binding matrix, ultrafiltration (purple) represents Amicon ultrafilter concentration and ultrafiltration and solids represents Amicon ultrafilter concentration with subsequent RNA extraction of isolated solids.

C) Relationship between wastewater input volume and DNA yield, defined as total ng of DNA per extraction. Column (pink) represents the 4S method using a silica column and Milk of Silica (salmon) represents the 4S method using a silicon dioxide binding matrix.

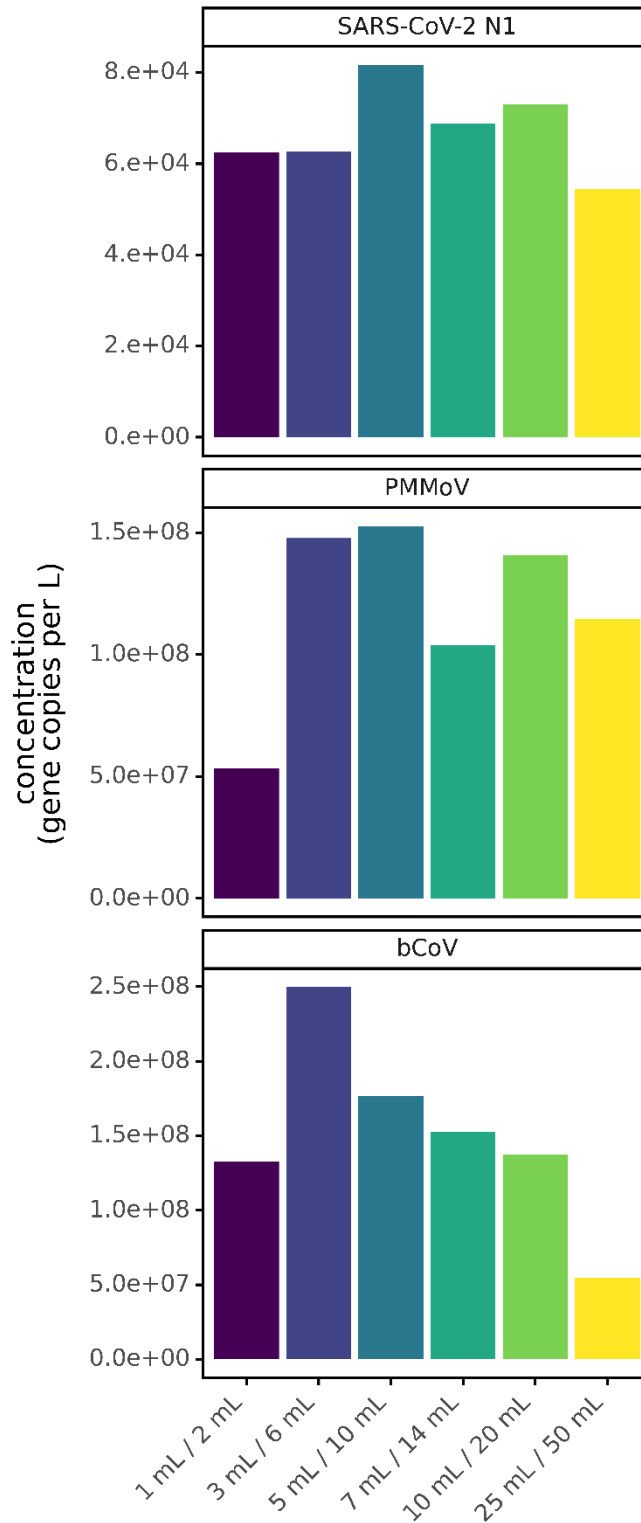


Figure S4. Impact of wash buffer volume use on SARS-CoV-2 N1, PMMoV and bCoV assay detection, reported in gene copies per liter. Volumes of wash buffer #1 and wash buffer #2 indicated on x-axis, n=1 extraction replicate per wash buffer volume used.

Tables

Table S1: Reaction conditions for each assay

Reaction Component	N1 Reaction concentration (μM)	PMMoV Reaction concentration (μM)	bCoV Reaction concentration (μM)	18S Reaction concentration (μM)
TaqMan Fast Virus 1-Step Master Mix*	1x	1x	1x	1x
Primer F	0.5	0.4	0.9	0.5
Primer R	0.5	0.4	0.9	0.5
Probe	0.12	0.2	0.25	0.13

*Plates 12, 16, and 17 used TaqPath 1-Step RT-qPCR Master Mix at the same concentration

Table S2: Thermocycling parameters for all assays

Thermocycling conditions		
Reaction Cycling Step	Temperature ($^{\circ}\text{C}$)	Time (minutes: seconds)
UNG incubation	25	2:00
RT step	50	15:00
Polymerase activation	95	2:00
45 cycles	95	0:03
	55	0:30

Table S3: qPCR assay information for the SARS-CoV-2 nucleocapsid N gene (N1), the bovine coronavirus transmembrane protein gene (bCoV), the pepper mild mottle virus coat protein gene (PMMoV) and human 18S ribosomal rRNA (18S)

Gene target	Type of Sequence (length; accession)	Sequence (5' -> 3')
N1	Forward primer	GACCCCAAAATCAGCGAAAT
	Reverse primer	TCTGGTTACTGCCAGTTGAATCTG
	Probe	FAM-ACCCCGCATTACGTTTGGTGGACC- MGB-NFQ
	Amplicon (72 bp; MN908947.3)	GACCCCAAAATCAGCGAAATGCACCCCGCATTACGTTTGGTGGACCCTCAGATTCAACTGGCAGTAACCAGA
PMMoV	Forward primer	GAGTGGTTTGACCTTAACGTTTGA
	Reverse primer	TTGTCGGTTGCAATGCAAGT
	Probe	FAM-CCTACCGAAGCAAATG-MGB-NFQ
	Amplicon (68 bp; AB716964)	GAGTGGTTTGACCTTAACGTTTGGAGCGGCCTACCGAAGCAAATGTCGCACTTGCATTGCAACCGACAA
bCoV	Forward primer	CTGGAAGTTGGTGGAGTT
	Reverse primer	ATTATCGGCCTAACATACATC
	Probe	FAM-CCTTCATATCTATACACATCAAGTTGTT- MGB-NFQ
	Amplicon (85 bp; AF39154)	CTGGAAGTTGGTGGAGTTCAACCCAGAAACAACAACCTTGATGTGTATAGATATGAAGGGAAGGATGTATGTTAGGCCGATAAT
18S	Forward primer	GGTTCCTTTGGTCGCTCGCT
	Reverse primer	GGGCTGACCGGGTTGGTTTT
	Probe	/56-FAM/AG AGC TAA T/ZEN/A CAT GCC GAC GGG C/3IABkFQ/
	Amplicon (138bp; 6G18 2)	GGTTCCTTTGGTCGCTCGCTCCTCTCCTACTTGGATAACTGTGGTAATTCTAGAGCTAATACATGCCGACGGGCGCTG ACCCCCTTCGCGGGGGGATGCGTGCATTTATCAGATCAAACCAACCCGGTCAGCCC

Table S4: RT-qPCR validation information

plate id	Target	linear dynamic range (orders of magnitude)	lowest quantity on the standard curve (Cq)	lowest quantity on the standard curve (gene copies per L)	lowest quantity on the standard curve (geometric standard deviation)	slope	y-intercept	R ²	PCR efficiency	Minimum Cq of NTC triplicates	intraassay variation (arithmetic mean of coefficient of variation of quantities on each plate)
12	N1	5	34.81	10	0.284	3.2	38.57	0.9917	1.05	negative	35.787
16	N1	5	36.04	20	0.083	3.5	41	0.9977	0.898	negative	30.353
17	PMMoV	6	35.01	1000	0.068	3.6	45.62	0.9988	0.893	negative	17.468
20	N1	6	34.93	10	0.271	3.4	38.38	0.9983	0.935	negative	22.521
21	N1	6	35.54	10	0.143	3.4	39.04	0.9995	0.946	negative	19.417
22	PMMoV	6	35.01	1000	0.124	3.8	47.39	0.9924	0.829	negative	10.092
23	PMMoV	6	35.59	1000	0.211	4.1	49.84	0.9494	0.745	negative	14.234
27	N1	6	34.46	10	0.364	3.3	38.09	0.9872	0.984	negative	19.871
28	PMMoV	4	29.47	10000	0.122	3.4	43.15	0.9995	0.955	39.03	15.694
32	bCoV	6	37.89	100	0.279	3.7	46.08	0.9956	0.837	negative	48.882
34	N1	6	36.84	10	0.04	3.3	40.21	0.9992	1.001	negative	4.469
35	bCoV	6	37.89	100	0.279	3.7	46.08	0.9956	0.837	negative	10.677
36	PMMoV	6	36.06	1000	0.104	4.2	50.4	0.9705	0.71	negative	10.078
37	N1	5	35.19	20	0.071	3.4	39.75	0.9997	0.953	negative	19.121
38	bCoV	6	37.89	100	0.279	3.7	46.08	0.9956	0.837	negative	16.418

						-						
39	PMMoV	6	34.46	1000	0.062	3.8	6	47.03	0.9842	0.816	negative	11.561
						-						
59	18S	6	29.36	1000	0.113	3.4	2	39.61	0.9999	0.962	37.73	12.657

Table S5: Evidence for LoD/LoQ

assay	standard curve Quantity (gene copies per reaction)	fraction of replicates positive	number of replicates that passed Grubbs test	number of replicates that failed Grubbs test	total number of replicates
N1	10	0.73	15	6	21
N1	20	0.89	18	0	18
N1	100	1	20	1	21
N1	1000	1	20	1	21
N1	10000	1	21	0	21
N1	100000	1	21	0	21
PMMoV	1000	1	15	0	15
PMMoV	10000	1	17	1	18
PMMoV	100000	1	17	1	18
PMMoV	1000000	1	16	2	18
PMMoV	10000000	1	18	0	18
PMMoV	100000000	1	15	0	15
bCoV	100	0.67	3	0	3
bCoV	1000	1	3	0	3
bCoV	10000	1	3	0	3
bCoV	100000	1	3	0	3
bCoV	1000000	1	3	0	3
bCoV	10000000	1	3	0	3
18S	1000	1	3	0	3
18S	10000	1	3	0	3
18S	100000	1	3	0	3
18S	1000000	1	3	0	3
18S	10000000	1	3	0	3
18S	100000000	1	3	0	3

Table S6: Reagent cost of the 4S method using a silica column or silicon dioxide particulate.

Material	4S-Column cost	4S “Milk-of-Silica” cost
50 mL tube	\$0.36	\$0.18
NaCl	\$0.48	\$0.48
Tris	\$0.02	\$0.02
EDTA	\$0.02	\$0.02
Bovilis Coronavirus Calf Vaccine	\$0.04	\$0.04
50 mL syringe	\$0.78	\$0.78
5uM 47mm PVDF membrane filter	\$1.56	\$1.56
Silicon Dioxide	N.A.	\$0.62
Zymo IIP columns with reservoir	\$8.41	N.A.
Ethanol (70%)	\$0.56	\$0.57
Ethanol (96%)	\$0.13	\$0.13
1.5 mL tube	\$0.02	\$0.02
1.5 mL Lo-bind tube	\$0.13	\$0.13
PCR water	NA	\$1.82
Isopropanol	NA	\$1.18
Sodium Acetate	NA	\$0.06
Elution Buffer (ZymoPURE)	\$0.31	\$0.31
Total Cost	\$12.83	\$7.93

Table S7: MIQE guideline essential information checklist

Requirement for submission	Requirement or location of requirement
Experimental Design	
Definition of experimental and control groups	Experimental groups defined as wastewaters purified via different extraction methods, with or without the addition of preservative salts.
Number within each group	Three wastewater RNA extraction replicates of an influent sample within each experimental group
Sample	
Description	Wastewater influent sample
Microdissection or macrodissection	Not applicable
Processing procedure	4S or ultrafiltration-based RNA extraction
If frozen, how quickly	Not applicable
If fixed, with what and how quickly	Not applicable
Sample storage conditions and duration	Samples stored for 1-2 days at 4°C or <2 weeks at -80°C
Nucleic Acid Extraction	
Procedure/instrumentation	“4S” purification using silica columns or silica particulate, Ultrafiltration as previously described, with subsequent AllPrep kit RNA extraction
Name of kit and details of modifications	Amicon 100kDA ultrafilter, AllPrep RNA/DNA extraction kit
Details of DNase or RNase treatment	Not applicable
Contamination assessment (DNA or RNA)	Not applicable
Nucleic acid quantification	Fluorescent dyes reactive to RNA and DNA
Instrument and method	Qubit4 fluorometer, high-sensitivity and broad-range RNA assay, broad-range DNA assay
RNA integrity: method/instrument	Not applicable
RIN/RQI or C _q of 3' and 5' transcripts	Not applicable
Inhibition testing	Spike and dilute method; RT-qPCR methods section
Reverse Transcription	
Complete reaction conditions	Table S1
Amount of RNA and reaction volume	5µL of extracted RNA and 20 µL reaction volume
Priming oligonucleotide and concentration	0.5uM- 0.9uM, detailed in table S1
Reverse transcriptase concentration	Included in TaqMan Fast Virus 1-Step Master Mix and TaqPath 1-Step RT-qPCR Master Mix (ThermoFisher Scientific)
Temperature and time	Table S2
qPCR target information	
Gene symbol	N – SARS-CoV-2 Nucleocapsid, RNA18S1 – RNA, 18S ribosomal 1, M – Membrane protein, bovine coronavirus, CP – PMMoV Coat protein
Sequence accession number	Table S3
Amplicon length	Table S3
In silico specificity screen	NCBI Primer-BLAST
Location of each primer by exon or intron	Not applicable
What splice variants are targeted	Not applicable

qPCR oligonucleotides	
Primer Sequences	Table S3
Location and identity of any modifications	Not applicable
qPCR protocol	
Complete reaction conditions	Table S1
Reaction volume and amount of cDNA	20 μ L, Not Applicable (1-Step RT-qPCR)
Primer, probe, Mg ²⁺ , and dNTP concentrations	Included in TaqMan Fast Virus 1-Step Master Mix and TaqPath 1-Step RT-qPCR Master Mix (ThermoFisher Scientific)
Polymerase identity and concentration	Included in TaqMan Fast Virus 1-Step Master Mix and TaqPath 1-Step RT-qPCR Master Mix (ThermoFisher Scientific)
Kit identity and manufacturer	RT-qPCR methods section
Additives	Not applicable
Complete thermocycling parameters	Table S2
Manufacturer of qPCR instrument	QuantStudio 3 Real-Time PCR system (ThermoFisher Scientific)
qPCR validation	
Specificity	No detected amplification of assays within negative RT-qPCR controls
For SYBR Green I, C _q of the NTC	Not applicable
Calibration curves with slope and y intercept	Table S4
PCR efficiency	Table S4
R ²	Table S4
Linear dynamic range	Table S4
C _q variation at LoD	Table S4
Evidence for LoD	Table S5
If multiplex, efficiency and LoD of each assay	Not applicable
Data Analysis	
qPCR analysis program	Custom Python pipeline; Data analysis methods section
Method of C _q determination	Automatic thresholding through Design and Analysis Software v1.5.1
Outlier analysis	Grubbs test; Data analysis methods section
Results for NTCs	Table S4
Justification of number and choice of reference genes for normalization method	Not applicable
Description of normalization method	Not applicable
Number and stage of technical replicates	RT-qPCR technical triplicates
Repeatability	Table S4
Statistical methods for results significance	Data analysis methods section
Software	Firmware v1.3.3, QuantStudio 3; Design and Analysis Software v1.5.1; QuantStudio 3

References

- (1) Haramoto, E.; Kitajima, M.; Kishida, N.; Konno, Y.; Katayama, H.; Asami, M.; Akiba, M. Occurrence of Pepper Mild Mottle Virus in Drinking Water Sources in Japan. *Appl. Environ. Microbiol.* **2013**, *79* (23), 7413–7418. <https://doi.org/10.1128/AEM.02354-13>.
- (2) Decaro, N.; Elia, G.; Campolo, M.; Desario, C.; Mari, V.; Radogna, A.; Colaianni, M. L.; Cirone, F.; Tempesta, M.; Buonavoglia, C. Detection of Bovine Coronavirus Using a TaqMan-Based Real-Time RT-PCR Assay. *Journal of Virological Methods* **2008**, *151* (2), 167–171. <https://doi.org/10.1016/j.jviromet.2008.05.016>.
- (3) Cao, Y.; Griffith, J. F.; Dorevitch, S.; Weisberg, S. B. Effectiveness of QPCR Permutations, Internal Controls and Dilution as Means for Minimizing the Impact of Inhibition While Measuring Enterococcus in Environmental Waters. *Journal of Applied Microbiology* **2012**, *113* (1), 66–75. <https://doi.org/10.1111/j.1365-2672.2012.05305.x>.
- (4) Bustin, S. A.; Benes, V.; Garson, J. A.; Hellemans, J.; Huggett, J.; Kubista, M.; Mueller, R.; Nolan, T.; Pfaffl, M. W.; Shipley, G. L.; Vandesompele, J.; Wittwer, C. T. The MIQE Guidelines: Minimum Information for Publication of Quantitative Real-Time PCR Experiments. *Clin Chem* **2009**, *55* (4), 611–622. <https://doi.org/10.1373/clinchem.2008.112797>.
- (5) Wu, F.; Zhang, J.; Xiao, A.; Gu, X.; Lee, W. L.; Armas, F.; Kauffman, K.; Hanage, W.; Matus, M.; Ghaeli, N.; Endo, N.; Duvallet, C.; Poyet, M.; Moniz, K.; Washburne, A. D.; Erickson, T. B.; Chai, P. R.; Thompson, J.; Alm, E. J. SARS-CoV-2 Titers in Wastewater Are Higher than Expected from Clinically Confirmed Cases. **2020**, *5* (4), 9.

- (6) Haramoto, E.; Malla, B.; Thakali, O.; Kitajima, M. First Environmental Surveillance for the Presence of SARS-CoV-2 RNA in Wastewater and River Water in Japan. *Sci Total Environ* **2020**, *737*, 140405. <https://doi.org/10.1016/j.scitotenv.2020.140405>.
- (7) Alameda County. Alameda County COVID-19 Daily Cumulative Cases by City, Place, and Zip Code https://data.acgov.org/datasets/5d6bf4760af64db48b6d053e7569a47b_3?page=10 (accessed Oct 22, 2020).
- (8) CCHS. Contra Costa COVID-19 Dashboard <https://www.coronavirus.cchealth.org/overview> (accessed Feb 11, 2021).